EPJ manuscript No.
(will be inserted by the editor)

Screened potential and quarkonia properties at high temperatures

J. Vijande[1,2], G. Krein[3], and A. Valcarce[1]

[1] Departamento de Física Fundamental, Universidad de Salamanca, E-37008 Salamanca, Spain
[2] Departamento de Física Atómica, Molecular y Nuclear e IFIC, Universidad de Valencia - CSIC, E-46100 Burjassot, Valencia, Spain
[3] Instituto de Física Teórica, Universidade Estadual Paulista, Rua Pamplona, 145 - 01405-900 São Paulo, SP, Brazil

Received: date / Revised version: date

Abstract. We perform a quark model calculation of the quarkonia $b\bar{b}$ and $c\bar{c}$ spectra using smooth and sudden string breaking potentials. The screening parameter is scale dependent and can be related to an effective running gluon mass that has a finite infrared fixed point. A temperature dependence for the screening mass is motivated by lattice QCD simulations at finite temperature. Qualitatively different results are obtained for quarkonia properties close to a critical value of the deconfining temperature when a smooth or a sudden string breaking potential is used. In particular, with a sudden string breaking potential quarkonia radii remain almost independent of the temperature up to the critical point, only well above the critical point the radii increase significantly. Such a behavior will impact the phenomenology of quarkonia interactions in medium, in particular for scattering dissociation processes.

PACS. 14.40.Lb Charmed mesons – 12.39.Jh Nonrelativistic quark model – 25.75.Nq Quark deconfinement – 24.85.+p Quarks, gluons, and QCD in nuclear reactions – 13.75.-n Low-energy hadron-hadron interactions

1 Introduction

The study of hot hadronic matter may yield a particularly clear picture of the physics of quark confinement [1]. At high temperatures, color screening may be strong enough to lead to the dissolution of quark-antiquark states [2]. Because of the large mass of the heavy quarks in charmonium and bottomonium, the velocity of the heavy quarks is small enough such that the binding effects in quarkonia at zero temperature might be understood in terms of a nonrelativistic potential. Color screening could then be masked in terms of in-medium modification of the interquark forces.

Nature of the confining potential has been a challenge for lattice QCD studies. Quenched and unquenched lattice QCD calculations were able to probe the linear raising potential between heavy color sources [3]. It has been also recently numerically investigated the transition of the static quark-antiquark string into a static-light meson-antimeson system, in other words string breaking in QCD [4]. These studies drove the idea of screening of the color forces at zero temperature as a consequence of the polarization of vacuum. This effect observed numerically should be enhanced in hot hadronic matter with observable consequences.

Recent publications [5,6] have emphasized the use of a screened potential in place of one linearly rising with inter-quark distance in a quark-model description of the hadronic spectrum. In these publications properties of heavy quarkonia ($c\bar{c}$ and $b\bar{b}$ bound states) such as masses, spin-spin splittings, leptonic widths and radiative decays have been calculated from a simple screened funnel quark potential model. Although the quality of the calculated spectra [5] is similar to that of other quark model calculations [7] that employ nonscreened confinement, important differences arise. The most salient ones are the finite number of quark-antiquark bound states and the pattern of energy differences of the higher excited states. The finiteness of the bound-state spectrum has interesting implications in the light-quark sector. In particular, the predicted [6] number of states is in almost perfect agreement with the experimentally observed states, a fact that might shed new light on the so-called missing resonance problem – for a recent review, see Ref. [8].

Screening of the potential is due to quark-antiquark creation from the vacuum as the interquark distance is increased and leads to the breaking of the color string that would be formed in the absence of sea quarks [3]. Such a string breaking has been confirmed in lattice QCD calculations [4]. It has also been suggested by the observation of nonlinear hadronic Regge trajectories [9]. A quite rapid crossover from a linear rising to a flat potential is well established in SU(2) Yang-Mills theories [10]. In addition, the mentioned recent lattice QCD calculations have also shown that the breaking is quite sudden, the $Q\bar{Q}$ potential saturates sharply for a breaking distance of the order of 1.25 fm corresponding to a saturation energy of

about twice the $B-$meson ($Q\bar{q}$) mass, indicating that the formation of two heavy-light subsystems $(B, \bar{B})$ is energetically favored. This information has been implemented in a quark model scheme [11] showing that, as a consequence of coupled channels above the physical thresholds (corresponding to the opening of decay channels), the description becomes progressively less accurate high in the spectrum. Moreover, the mixing with the continuum can also modify the short-range part of the interaction. Nonetheless, an effective (renormalized) nonscreened potential continues being useful up to energies not too far above the lowest physical threshold. At sufficiently high baryon densities and/or temperatures, one would expect that such a screening would be even stronger.

However, recent results of lattice QCD simulations of charmonium correlation functions at finite temperature have shown some rather unexpected results [12,13,14]. The spectral functions in some channels display narrow peaks at temperatures T well above the deconfinement temperature T_c. Peaks in these mesonic correlation functions indicate that the quark and the antiquark are strongly correlated, leading to the interpretation that bound states of the heavy charm quarks can possibly survive above the deconfinement temperature. The results came to a surprise since early expectations [1] were that $c\bar{c}$ bound states (like the J/Ψ) would dissolve already at temperatures close to T_c.

These lattice results have stirred renewed interest [15, 16,17,18,19,20] in incorporating finite temperature effects in a potential model. There is a long history [21] on the use of temperature-dependent potentials in a Schrödinger equation to study quarkonium properties at finite temperatures and the tlattice results have brought new physical insight into the problem. Recent studies have attempted to incorporate this insight into the phenomenology of the modified potentials. Within these approaches a temperature dependence for the potential is extracted from lattice results for the finite temperature free energy of a static quark-antiquark pair. A problem with such an strategy is that the free-energy is not itself a potential energy since it contains an entropy contribution. One consequence of such a parametrization of the binding potential is that entropy smooths out any sudden breaking of the string. This in turn has the effect that quarkonia properties close to the critical temperature have a smooth temperature dependence.

Although at the moment such a finite temperature quark model, contrary to the zero temperature case, cannot be justified as some limiting approximation that follows from a systematic effective field theory, it does seem to provide a simple phenomenological attempt to bring insight into the problem. At zero temperature, potential models for quarkonia can be derived in QCD from first principles as the leading order approximation of an effective field theory known as potential nonrelativistic QCD [3, 22]. A finite temperature generalization of this approach has been attempted only very recently [23], but no string breaking is accessible in such an approach. Work on similar grounds to obtain a finite temperature potential to be used in a Schrödinger equation was done in Ref. [24]

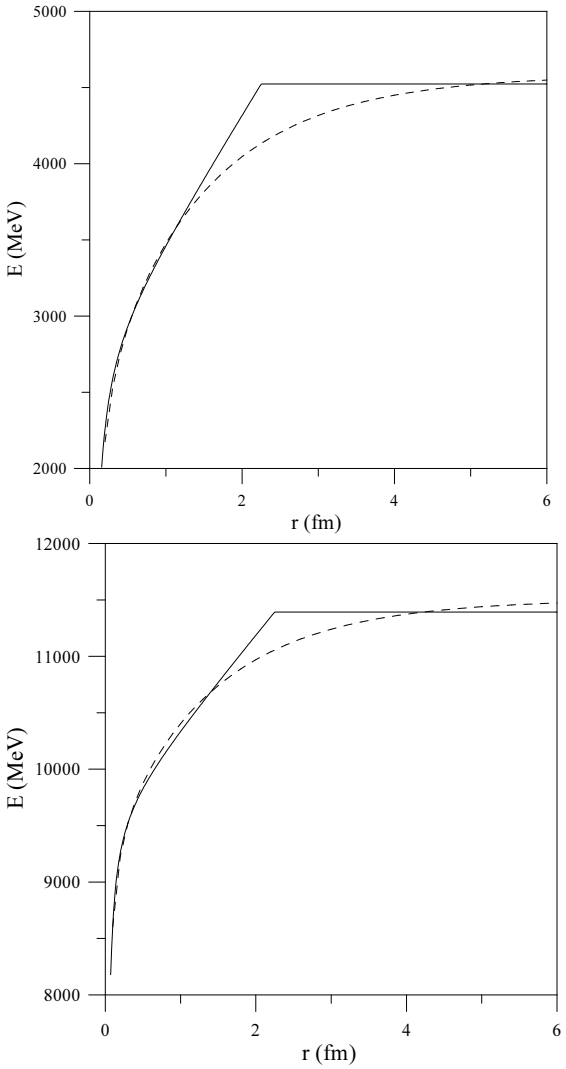

Fig. 1. Smooth and sudden potentials for charmonium (upper panel) and bottomonium (lower panel) pseudoscalar S wave states. In all cases the value of the corresponding constituent quark masses ($2m_c$ or $2m_b$) has been added.

The purpose of the present paper is to show that one obtains qualitatively different behavior of quarkonia properties close to the critical temperature when a sudden string-breaking potential is used. In particular, the radius of a quarkonium bound state remains almost independent of the temperature up to the critical temperature, when starts to increase abruptly. Such a behavior will impact the phenomenology of quarkonia interactions in medium, in particular for scattering dissociation processes [25,26, 27,28], a topic very important for the experimental programs of heavy-ion collisions like the experiments at the FAIR facility at the GSI laboratory in Germany, in particular for the CBM experiment [29].

The paper is organized as follows. In the next section we discuss the models incorporating smooth and sudden breaking at zero and finite temperature and we present

Table 1. $T = 0$ parameters.

	Smooth	Sudden
σ (MeV fm^{-1})	1470	800
μ (fm^{-1})	0.71	–
$1/r_b$ (fm^{-1})	–	0.44
α (MeV fm)	96	106
r_0 (fm)	0.38	0.36
m_c (MeV)	1264	1385
m_b (MeV)	4724	4820

our numerical results. A model for the temperature dependence of the screening parameters is discussed in Section 3. Conclusions and Perspectives are summarized in Section 4.

2 Smooth versus sudden string breaking

Our approach in the present paper will be purely phenomenological. Initially, for the purposes of investigating the consequences of sudden string breaking at finite temperatures it is not necessary to adopt any specific model for the temperature dependence of screening parameters. We will calculate the spectrum of charmonium and bottomonium using two different potentials, one with smooth string breaking and another with sudden string breaking. We then vary the screening parameters and investigate its effect over the energies, radii and decay constants. In the next section we will discuss possible relations of our phenomenological approach to different models that parametrize the temperature dependence of the screening parameters. This will allow us to relate changes of the observables with temperature.

We implement smooth string breaking in the potential as

$$V_{smooth}(r) = \frac{\sigma}{\mu}\left(1 - e^{-\mu r}\right) + V_{OGE}(r), \qquad (1)$$

where $V_{OGE}(r)$ is the one-gluon exchange (OGE) potential given by

$$V_{OGE}(r) = -\frac{\alpha}{r} + \alpha \frac{\hbar^2}{m_q m_{\bar{q}}} \frac{e^{-r/r_0}}{r r_0^2} \left(\boldsymbol{\sigma}_1 \cdot \boldsymbol{\sigma}_2\right). \qquad (2)$$

Here σ and α are phenomenological parameters to be fixed by fitting the quarkonium spectrum, and the delta function of the OGE spin-spin part has been smoothed out with a parameter r_0. The asymptotic limit $r \to \infty$ of the potential is a constant, given by

$$V_{smooth}(r \to \infty) = \frac{\sigma}{\mu}. \qquad (3)$$

Sudden string breaking is implemented as

$$V_{sudden}(r) = \begin{cases} \sigma\, r + V_{OGE}(r), & r < r_b \\ \sigma r_b + V_{OGE}(r_b), & r \geq r_b\,. \end{cases} \qquad (4)$$

Table 2. $c\bar{c}$ bound state masses (in MeV) with smooth and sudden string breaking at $T = 0$ up to four radial excitations. Experimental masses taken from the PDG [32].

State (nL_{2S+1})	M_{smooth}	M_{sudden}	M_{exp}
$1S_1$	2979	2976	2979.8 ± 1.2
$1S_3$	3099	3096	3096.916 ± 0.011
$1P_1$	3491	3453	3525.93 ± 0.27
$1P_3$	3521	3482	3493.87
$2S_1$	3639	3600	3637 ± 4
$2S_3$	3686	3654	3686.093 ± 0.034
$1D_1$	3790	3745	
$1D_3$	3801	3757	3772.4 ± 1.1
$2P_1$	3907	3897	
$2P_3$	3923	3917	3929 ± 5
$3S_1$	4008	4028	
$3S_3$	4035	4067	4039 ± 1
$2D_1$	4098	4128	
$2D_3$	4105	4138	4153 ± 3
$3P_1$	4178	4266	
$3P_3$	4189	4282	
$4S_1$	4248	4384	
$4S_3$	4265	4413	4421 ± 4
$3D_1$	4307	4458	
$3D_3$	4312	4467	
$4P_1$	4361	–	
$4P_3$	4368	–	

The asymptotic limiting value of this potential is spin(S)-dependent and it is given by

$$V_{sudden}(r \to \infty) = \sigma r_b - \frac{\alpha}{r_b} + \left[S(S+1)\right] \alpha \frac{\hbar^2}{m_q m_{\bar{q}}} \frac{e^{-r_b/r_0}}{r_0^2 r_b}. \qquad (5)$$

We adjust parameters to obtain a reasonable description of the lowest states. Although they are effective parameters they are not unphysical, see Ref. [30] for a detailed discussion of their value. Their values are given in Table 1 (we refer to these as the $T = 0$ parameters). In Fig. 1 we plot the potentials for the S wave pseudoscalar (spin equal to zero) states of charmonium and bottomonium. The differences between the smooth and sudden string-breaking potentials are concentrated in the region of $r \simeq 2$ fm. We have solved the Schrödinger equation for the above potentials for charmonium and bottomonium using standard Numerov techniques [31]. Our results, together with the available experimental values taken from the PDG [32] are shown in Tables 2 and 3. Many of the experimental results shown in the tables have no definite assignment of orbital angular momentum. Therefore, we have identified the states guided by the results of our model. As a general trend, one sees that the higher orbital excitations are better described by a sudden breaking potential. This important result, already observed in the baryon spectra [6], imply that these states are very sensitive to the form of the confining potential and as such they will be an ideal benchmark to provide clues on the nature of the screening behavior of the potential.

Table 3. $b\bar{b}$ bound state masses (in MeV) with smooth and sudden string breaking at $T = 0$ up to six radial excitations. Experimental masses taken from the PDG [32].

State (nL_{2S+1})	M_{smooth}	M_{sudden}	M_{exp}
$1S_1$	9434	9432	
$1S_3$	9459	9463	9460.30 ± 0.26
$1P_1$	9951	9929	
$1P_3$	9958	9936	9888.1
$2S_1$	10059	10012	
$2S_3$	10068	10022	10023.26 ± 0.31
$1D_1$	10218	10167	
$1D_3$	10221	10171	10161.1 ± 1.7
$2P_1$	10320	10263	
$2P_3$	10324	10267	10252.2
$3S_1$	10404	10339	
$3S_3$	10409	10345	10355.2 ± 0.5
$2D_1$	10502	10441	
$2D_3$	10505	10443	
$3P_1$	10583	10528	
$3P_3$	10586	10531	
$4S_1$	10651	10599	
$4S_3$	10655	10604	10579.4 ± 1.2
$3D_1$	10721	10677	
$3D_3$	10722	10678	
$4P_1$	10787	10758	
$4P_3$	10789	10760	
$5S_1$	10843	10825	
$5S_3$	10846	10829	10865 ± 8
$4D_1$	10895	10889	
$4D_3$	10896	10891	
$5P_1$	10949	10966	
$5P_3$	10951	10968	
$6S_3$	10998	11034	11019 ± 8

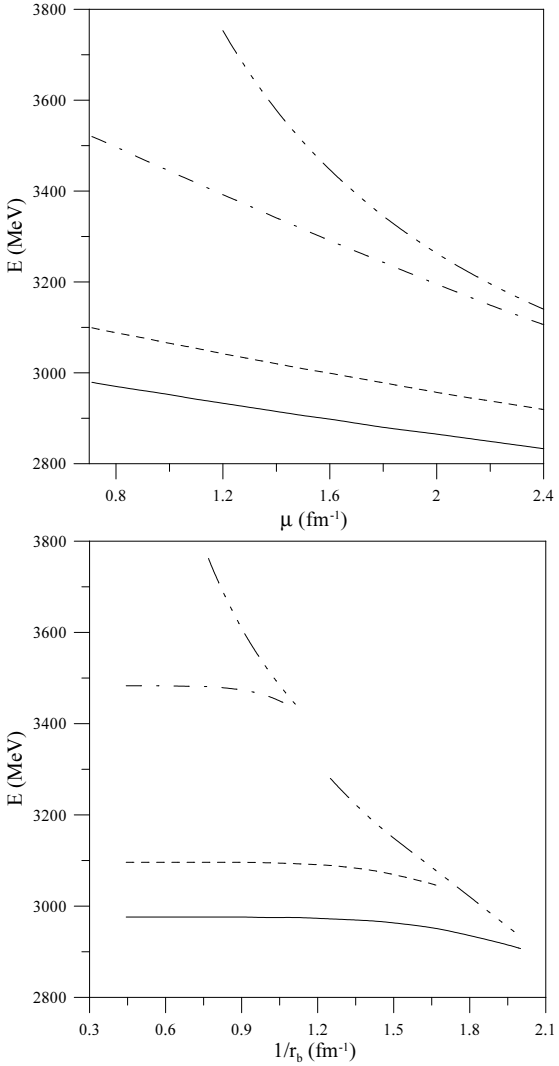

Fig. 2. η_c (solid), J/Ψ (dashed) and χ_{cJ} (dashed-dotted) energies as a function of the smooth μ (upper panel) and sudden $1/r_b$ (lower panel) screening parameters. The dashed–triple-dotted curve shows the threshold energies of these states.

Next we keep all parameters fixed and vary the screening parameters μ and $1/r_b$ so to mimic a temperature dependence. Here we do not use a specific model for the temperature dependence of these parameters, this will be discussed in the following section. Results for the total energy E and r.m.s. radius $\sqrt{\langle r^2 \rangle}$ of the lowest S and P wave states of charmonium as functions of the smooth (μ) and sudden ($1/r_b$) screening parameters are shown respectively in Figs. 2 and 3. The corresponding results for bottomonium are shown Figs. 4 and 5. In Tables 4 and 5 the results corresponding to the sudden potential are presented together with the threshold energies E_{th} and wavefunctions at the origin $\phi(0)$.

The results are quite striking. The observables calculated with a smooth screening or with sudden screening behave dramatically different as the corresponding screening parameters are varied. While the observables calculated with smooth screening vary continuously as μ is increased, the observables calculated with sudden screening change very little as $1/r_b$ increases, until a critical value of this parameter is reached when they change abruptly. Such an abrupt change on observables at a critical value of $1/r_b$ naturally leads to the interpretation of a phase transition, the deconfinement transition. Of course, related to this critical value of $1/r_b$ there should be a critical temperature T_c.

As mentioned in the introduction, an abrupt increase of the size of the meson wave functions will impact the phenomenology of quarkonia interactions in medium, in particular for scattering dissociation processes [25,26,27, 28,29]. In a quark model description, such dissociation cross sections depend upon the degree of overlap of the wave functions of the hadrons and so depend crucially on the size of the wave functions in coordinate space. The diagram shown in Fig. 6 illustrates such a process for the case of a meson-meson process. The figure illustrates a process in which two mesons m_1 and m_2 collide and give in general two different mesons m_3 and m_4. The basic mechanism here is quark-gluon interchange in which the two quarks, one from each of the colliding mesons, are interchanged with each other leading to a final state that is different from the initial one. A typical and very impor-

Table 4. Values of the threshold E_{th} and total E energies, in MeV, r.m.s. radius $\sqrt{\langle r^2\rangle}$, in fm, and wavefunction at the origin $\phi(0)$, in fm$^{-3/2}$, of the lowest charmonium S and P wave states for different values of the sudden screening parameter $1/r_b$, in fm^{-1}.

	η_c				J/Ψ				χ_{cJ}			
$1/r_b$	E_{th}	E	$\sqrt{\langle r^2\rangle}$	$\phi(0)$	E_{th}	E	$\sqrt{\langle r^2\rangle}$	$\phi(0)$	E_{th}	E	$\sqrt{\langle r^2\rangle}$	$\phi(0)$
0.44	4523	2976.0	0.4066	13.328	4523	3096.4	0.4596	9.486	4534	3482.6	0.7126	0
0.48	4399	2976.0	0.4066	13.328	4399	3096.4	0.4596	9.486	4412	3482.6	0.7126	0
0.53	4234	2976.0	0.4066	13.328	4234	3096.4	0.4596	9.486	4250	3482.6	0.7126	0
0.59	4067	2976.0	0.4066	13.328	4068	3096.4	0.4596	9.486	4087	3482.6	0.7129	0
0.67	3899	2976.0	0.4066	13.328	3900	3096.4	0.4597	9.486	3924	3482.4	0.7145	0
0.77	3727	2975.8	0.4067	13.328	3729	3096.3	0.4600	9.484	3762	3481.1	0.7235	0
0.91	3552	2975.7	0.4076	13.320	3554	3096.0	0.4624	9.468	3600	3473.1	0.7773	0
1.00	3461	2975.4	0.4093	13.305	3465	3095.3	0.4664	9.439	3521	3461.4	0.8892	0
1.11	3368	2974.6	0.4132	13.262	3374	3093.5	0.4759	9.363	3443	3432.1	1.4710	0
1.25	3271	2972.4	0.4230	13.151	3280	3088.9	0.4998	9.170	Melted			
1.43	3168	2966.5	0.4483	12.856	3182	3077.0	0.5661	8.669	Melted			
1.67	3058	2950.6	0.5207	12.070	3078	3046.3	0.8268	7.260	Melted			
2.00	2933	2906.7	0.8556	9.633	Melted				Melted			
2.50	Melted				Melted				Melted			

Table 5. Values of the threshold E_{th} and total E energies, in MeV, r.m.s. radius $\sqrt{\langle r^2\rangle}$, in fm, and wavefunction at the origin $\phi(0)$, in fm$^{-3/2}$, of the lowest bottomonium S and P wave states for different values of the sudden screening parameter $1/r_b$, in fm^{-1}.

	η_b				$\Upsilon(1S)$				χ_{bJ}			
$1/r_b$	E_{th}	E	$\sqrt{\langle r^2\rangle}$	$\phi(0)$	E_{th}	E	$\sqrt{\langle r^2\rangle}$	$\phi(0)$	E_{th}	E	$\sqrt{\langle r^2\rangle}$	$\phi(0)$
0.44	11392	9432.2	0.2077	41.530	11393	9462.8	0.2136	39.271	11396	9936.0	0.4095	0
0.48	11269	9432.2	0.2077	41.530	11270	9462.8	0.2136	39.271	11273	9936.0	0.4095	0
0.53	11104	9432.2	0.2077	41.530	11104	9462.8	0.2136	39.271	11109	9936.0	0.4095	0
0.67	10769	9432.2	0.2077	41.530	10769	9462.8	0.2136	39.271	10776	9936.0	0.4095	0
0.91	10423	9432.2	0.2077	41.530	10424	9462.8	0.2136	39.271	10437	9936.0	0.4096	0
1.11	10242	9432.2	0.2077	41.530	10242	9462.8	0.2136	39.271	10262	9935.9	0.4105	0
1.43	10048	9432.2	0.2078	41.528	10049	9462.8	0.2137	39.266	10082	9933.3	0.4265	0
1.67	9942	9432.1	0.2081	41.513	9944	9462.7	0.2141	39.250	9989	9924.6	0.4810	0
1.82	9886	9432.0	0.2086	41.487	9888	9462.5	0.2147	39.250	9941	9912.9	0.5859	0
2.00	9826	9431.6	0.2098	41.423	9829	9462.1	0.2162	39.145	Melted			
2.50	9692	9428.6	0.2181	40.922	9696	9458.5	0.2263	38.566	Melted			
3.33	9521	9408.8	0.2634	38.059	9529	9436.5	0.2829	35.318	Melted			
4.00	9408	9370.8	0.3893	32.075	9419	9393.3	0.4590	28.454	Melted			
4.26	9368	9348.6	0.5144	28.194	Melted				Melted			
5.00	Melted				Melted				Melted			

tant example is the process $J/\Psi + \pi \to D\bar{D}^*$. It is clear that the constituent interchange will only happen when there is significant overlap between the wave functions of two mesons. The same quark-gluon interchange mechanism is also present in elastic hadron-hadron scattering and has been used in recent publications to describe the short-range part of several different processes [28,33]. As in dissociation processes, the elastic processes are also very sensitive to the sizes of the wave functions of the colliding hadrons.

In order to illustrate the effect of an abrupt increase of the size of the wave functions on a cross section, let us consider quark-gluon interchange in elastic meson-meson scattering. To evaluate the cross-section, we use the quark-Born-diagram method [34,35], which provides a good approximation [25] to a more complete resonating group method or Born-Oppenheimer calculation [36]. There are several diagrams that contribute to this process, being that shown in Fig. 6 a representative one. The evaluation of such graphs requires the quark-gluon interaction and the hadron wave functions. The calculation of these diagrams can be carried out analytically when one uses Gaussian forms for the hadron wave functions and a contact interaction for the quark-quark interaction (the wavy line in Fig. 6). To set the notation, let the internal meson wave functions $\psi(r)$ be given as (for equal quark masses)

$$\psi(r) = \left(\frac{1}{2\pi}\right)^{3/2} \left(\frac{\pi}{\lambda}\right)^{3/4} e^{-r^2/8\lambda}, \tag{6}$$

so that the r.m.s. radius of the meson is given by $\langle r^2\rangle = 6\,\lambda$. In general, as the c.m. total energy of the meson-

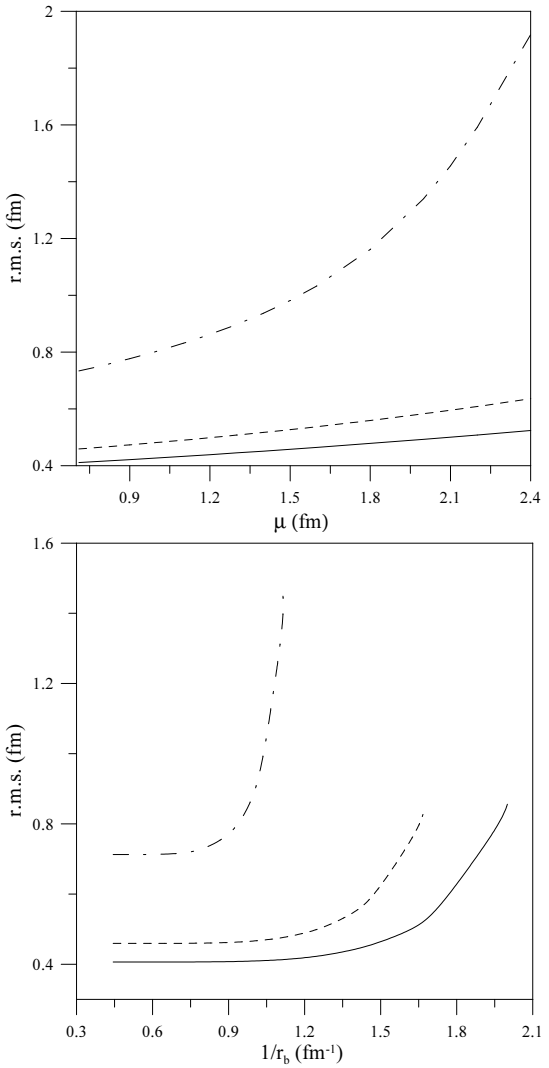

Fig. 3. η_c (solid), J/Ψ (dashed) and χ_{cJ} (dashed-dotted) r.m.s. as a function of the smooth μ (upper panel) and sudden $1/r_b$ (lower panel) screening parameters.

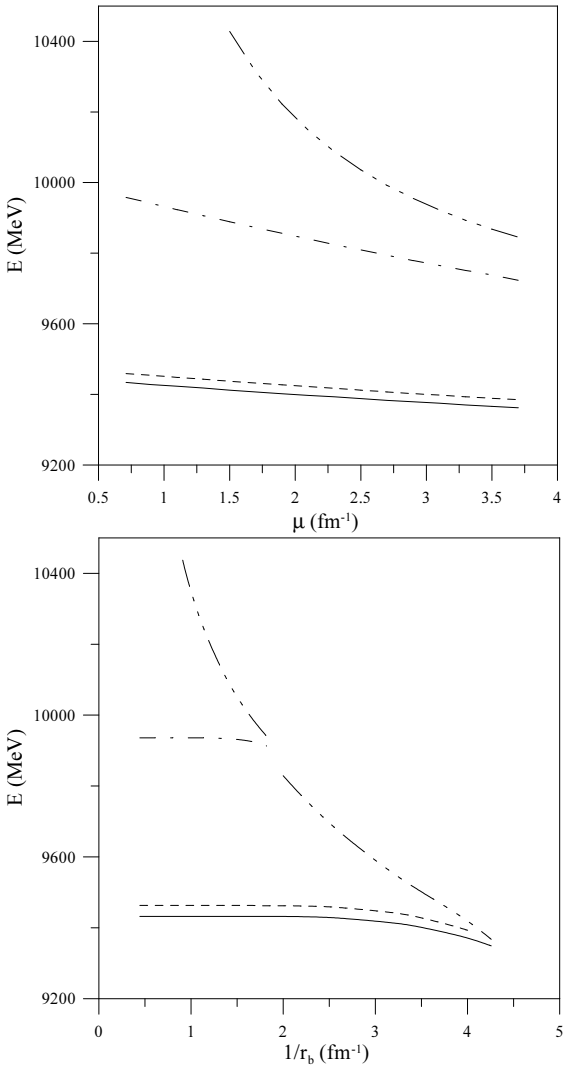

Fig. 4. η_b (solid), $\Upsilon(1S)$ (dashed) and χ_{bJ} (dashed-dotted) energies as a function of the smooth μ (upper panel) and sudden $1/r_b$ (lower panel) screening parameters. The dashed–triple-dotted curve shows the threshold energies of these states.

meson system s is increased, most of the Born elastic cross section decreases very rapidly and leaves a constant cross section at high energies, when $s \gg 1/\lambda$ – see discussions in Ref. [34]. Specifically, the behavior of the cross section at large s is given by

$$\lim_{s\gg 1/\lambda} \sigma \sim \frac{1}{\lambda} \sim \frac{1}{\langle r^2 \rangle}. \tag{7}$$

On the other hand, at low momentum transfers t such that t/s is small, the differential cross section behaves as

$$\lim_{t/s\ll 1} \frac{d\sigma}{dt} \sim \frac{1}{\lambda} e^{\lambda t}. \tag{8}$$

Although these results are for the case when all meson wave functions have the same size λ, they are of general validity. The final expression would be more complicated when meson wave functions of different sizes are used, but the behavior of the above cross section would be qualitatively the same, in that they decrease when the size of any of the meson wave functions increases.

From Eqs. (7) and (8) it is evident the role played by the size of the meson wave functions. When the size of the wave functions increase abruptly as the confining string breaks, the high energy cross sections that involve constituent interchange will change abruptly. As the critical point is crossed, the model discussed here predicts that the cross sections involving charmonium can decrease by a factor of five before the hadrons melt. For bottomonium the decrease is a factor of two.

The physical reason for the decrease of the cross sections is of course due to the fact that the hadron wave functions flatten out as their size parameters increase, since they are normalized. As the hadron wave functions flatten out, the overlap of the wave functions of the colliding hadrons is less significative and as such the probability

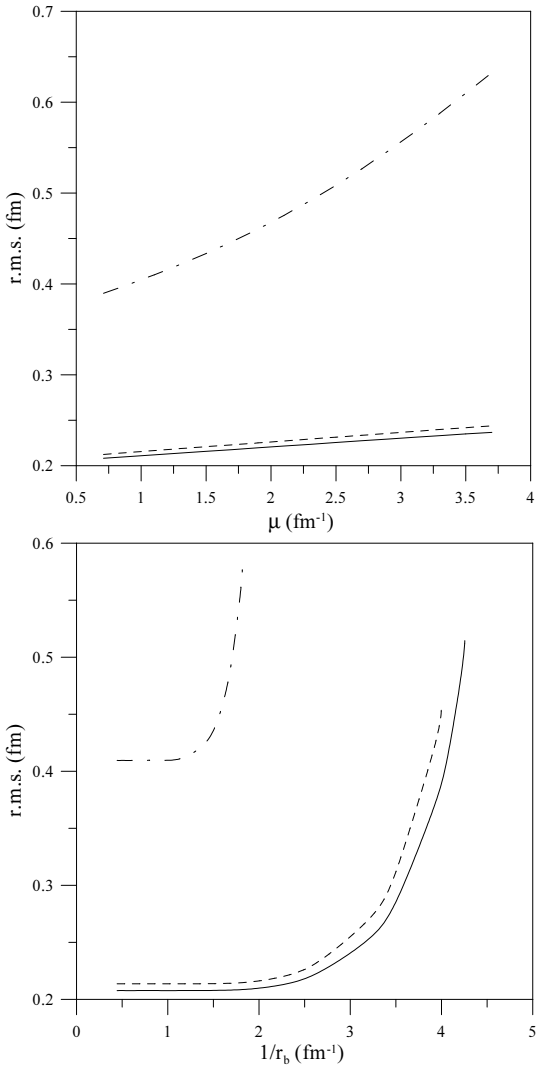

Fig. 5. η_b (solid), $\Upsilon(1S)$ (dash) and χ_{bJ} (dash-dot) r.m.s. as a function of the smooth μ (upper panel) and sudden $1/r_b$ (lower panel) screening parameters.

of constituent interchange is smaller. This effect is similar to the decrease of the electroweak decay constants as the size parameter increases. Since the decay constants are proportional to the wave function at the origin $\phi(0)$, they will decrease because $\phi(0)$ decreases as the extension of the wave function increases – see Tables 4 and 5.

3 A model for the temperature dependence of screening parameters

A phenomenological relation between the sreening parameters, μ in Eq. (1) or r_b in Eq. (4), with temperature can be made within the approach of Ref. [5], where the screening parameter is connected to an effective gluon mass scale in the infrared. Although a particular framework will be used to substantiate this, we trust that it might be of general validity. Suppose initially that the heavy-quark potential in coordinate space is defined as the Fourier transform

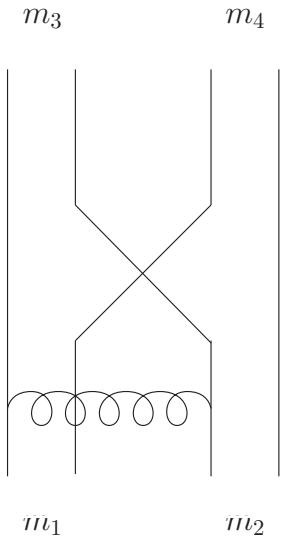

Fig. 6. Pictorial representation of the constituent interchange mechanism in meson-meson scattering.

of the static one-gluon-exchange with a running coupling constant $\alpha_s(Q^2)$. For the sake of argument, let us suppose [5] that $\alpha_s(Q^2)$ is given by the form derived in QCD by Cornwall long ago [37], namely

$$\alpha_s(Q^2) = \frac{4\pi}{\beta_0 \ln\left[(Q^2 + 4M_g^2(Q^2))/\Lambda^2\right]}, \qquad (9)$$

where $\beta_0 = (33-2n_f)/3$, n_f is the number of quark flavors with masses much smaller than Q, $\Lambda \sim 300$ MeV is the QCD scale parameter, and $M_g(Q^2)$ is an effective running gluon mass given by

$$M_g^2(Q^2) = m_g^2 \left(\frac{\ln\left[(Q^2+4m_g^2)/\Lambda^2\right]}{\ln\left(4m_g^2/\Lambda^2\right)}\right)^{-12/11}, \qquad (10)$$

with m_g being a constant mass scale and is responsible for the existence of confinement. One has that $\alpha_s(Q^2)$ runs from 0 in the ultraviolet asymptotic freedom limit $Q^2 \to \infty$, to $\alpha(0) = 4\pi/\beta_0 \ln(4m_g^2/\Lambda^2)$ in the deep infrared limit of $Q^2 \to 0$. Now, for $M_g^2(Q^2) \sim \Lambda^2$ one obtains a linearly-rising potential in coordinate space, since in this limit $\alpha_s(Q^2) \to 1/Q^2$. Strictly speaking this occurs for the precise value $M^2(Q^2) = \Lambda^2/4$, otherwise the potential is not exactly linear, but still absolutely confining. Therefore, the potential one gets is of Coulomb type at short distances (modified by asymptotic freedom) and confining at long distances. Obviously, both short- and long-distance components of this potential do not contain the effects of screening. However, screening can be modeled by modifying the potential so that its long distance component saturates at a distance $1/\mu$, where μ is a screening mass. Screening goes away for $\mu = 0$ and the purely confining potential with $M_g \sim \Lambda$ is recovered. In view of the interplay between μ and M_g it is natural to propose [5],

$$\mu = \Lambda - M_g\,. \qquad (11)$$

These effects were parametrized in exploratory lattice studies by a screened funnel potential [38]. Although this parametrization does not reproduce the rapid turnover around 1 fm from linearly rising to flat potential suggested by modern lattice results [39], we will follow it for the sake of simplicity. For a meson the above reasoning would give rise to a confining static potential of the form

$$V_{conf}(r) = \frac{\sigma}{\mu} - \sigma r \frac{e^{-\mu r}}{\mu r} = \frac{\sigma}{\mu} - \sigma r \left[\frac{e^{-(\Lambda - M_g(Q_0^2))r}}{(\Lambda - M_g(Q_0^2))r} \right] \tag{12}$$

where Q_0 is the running scale of μ. In this equation the relation between μ and M_g has been made explicit. This identification establishes a deep connection between the saturation of the coupling constant and the interquark pair creation mechanism both effects governed by $M_g(Q_0^2)$. Therefore μ runs with Q_0^2 so that $0 \simeq \mu(Q_0^2 = 0) \leq \mu(Q_0^2) \leq \mu(Q_0^2 \to \infty) \simeq 1.52\ \mathrm{fm}^{-1}$. In this approach, finite temperature effects can be introduced in the potential by making the effective running gluon mass temperature dependent, in such a way that for large temperatures confinement would disappear. This would imply $M_g^2(Q_0^2, T)$ must decrease with temperature for a fixed value of Q_0^2. Thus, the temperature dependence translates into the screening parameter through Eq. (11), that could now be written as

$$\mu(Q_0^2, T) = \Lambda - M_g(Q_0^2, T) \tag{13}$$

giving rise to a screening parameter μ increasing with temperature. Assuming that the scale dependence of M_g at finite temperature is still similar to Eq. (10) and making use of Eq. (13), one can obtain the temperature dependence of the screening parameter. Finally, making use of the typical momentum of charmonium that could be assimilated to its reduced mass, one can then obtain $\mu(Q_c^2, T) = \mu_c(T)$ appropriate for charmonium. Similar conclusions were obtained in Refs. [21,40]. In particular, Ref. [40] assumed a linear dependence of μ on T as obtained in first lattice estimates of screening in high temperature SU(N) gauge theory.

The above reasoning could be repeated for a rapid turnover transition potential as that of Eq. (4) obtaining the same conclusions. Admittedly this is a very crude way to obtain the temperature dependence of the gluon mass scale, it does seem to make physical sense, in view of the expectation that confinement goes away at sufficiently high temperatures.

4 Conclusions and outlook

To summarize, we have performed a detailed quark model calculation of the $b\overline{b}$ and $c\overline{c}$ sectors at zero and finite temperature comparing results obtained using smooth and sudden string breaking potentials. The scale- and temperature-dependence of the screening parameters μ and $1/r_b$ has been discussed. Such a dependence has been motivated by lattice QCD simulations at finite temperature. The properties of quarkonia close to the critical deconfining temperature depend strongly on the choice made for the screening, sudden or smooth. When a sudden string breaking potential is preferred, mesons are unaffected by the temperature increase up to the vicinity of the critical temperature T_c. Once this temperature is exceeded the radii increases suddenly and the energies and wave functions close to the origin drop. As opposed to this, when a smooth screening potential is considered meson properties respond to any modification in the temperature in a continuous way, and therefore reacting even to small changes of the temperature. Such a different behavior will modify drastically the phenomenology of quarkonia interactions in medium, in particular for scattering dissociation processes. Heavy-ion collision experiments, like FAIR at GSI, are ideally suited to discriminate between both possibilities and therefore to provide an important ingredient in order to clearly specify the *long range* (≈2 fm) structure of confinement.

This work has been partially funded by the Spanish Ministerio de Educación y Ciencia and EU FEDER under Contracts No. FPA2007-65748 and PCI2005-A7-0312, by Junta de Castilla y León under Contract No. SA016A17, and by the Spanish Consolider-Ingenio 2010 Program CPAN (CSD2007-00042). Partial financial support by the Brazilian agencies CNPq and FAPESP is also acknowledged.

References

1. T. Matsui, H. Satz, Phys. Lett. B **178**, 416 (1986).
2. A. Mócsy, P. Petreczky, Phys. Rev. D **77**, 014501 (2008).
3. G. S. Bali, Phys. Rep. **343**, 1 (2001).
4. G. S. Bali, H. Neff, T. Duessel, T. Lippert, K. Schilling [SESAM Collaboration], Phys. Rev. D **71**, 114513 (2005).
5. P. González, A. Valcarce, H. Garcilazo, J. Vijande, Phys. Rev. D **68**, 034007 (2003).
6. J. Vijande, P. González, H. Garcilazo, A. Valcarce, Phys. Rev. D **69**, 074019 (2004).
7. E. Eichten, K. Gottfried, T. Kinoshita, K. D. Lane, T. M. Yan, Phys. Rev. D **21**, 203 (1980).
8. S. Capstick, W. Roberts, Prog. Part. Nucl. Phys. **45**, S241 (2000).
9. M. M. Brisudová, L. Burakovsky, T. Goldman, Phys. Rev. D **61**, 054013 (2000).
10. P. W. Stephenson, Nucl. Phys. B **550**, 427 (1999).
11. E. S. Swanson, J. Phys. G **31**, 845 (2006).
12. T. Umeda, K. Nomura, H. Matsufuru, Eur. Phys. J. C **39S1**, 9 (2005).
13. M. Asakawa, T. Hatsuda, Phys. Rev. Lett. **92**, 012001 (2004).
14. S. Datta, F. Karsch, P. Petreczky, I. Wetzorke, Phys. Rev. D **69**, 094507 (2004).
15. E. V. Shuryak, I. Zahed, Phys. Rev. C **70**, 021901 (2004).
16. E. V. Shuryak, I. Zahed, Phys. Rev. D **70**, 054507 (2004).
17. C. Y. Wong, Phys. Rev. C **72**, 034906 (2005).
18. W. M. Alberico, A. Beraudo, A. de Pace, A. Molinari, Phys. Rev. D **72**, 114011 (2005).
19. M. Mannarelli, R. Rapp, Nucl. Phys. A **774**, 761 (2006).
20. A. Mócsy, P. Petreczky, Phys. Rev. D **73**, 074007 (2006).
21. H. Satz, J. Phys. G **32**, R25 (2006).
22. N. Brambilla, A. Pineda, J. Soto, A. Vairo, Rev. Mod. Phys. **77**, 1423 (2005).

23. M. Laine, O. Philipsen, M. Tassler, JHEP **0709**, 066 (2007); M. Laine, JHEP **0705**, 028 (2007); M. Laine, O. Philipsen, P. Romatschke, M. Tassler, JHEP **0703**, 054 (2007).
24. N. Brambilla, J. Ghiglieri, A. Vairo, P. Petreczky, Phys. Rev. D **78**, 014017 (2008).
25. D. Hadjimichef, G. Krein, S. Szpigel, J. S. da Veiga, Ann. Phys. **268**, 105 (1998).
26. C. Y. Wong, E. S. Swanson, T. Barnes, Phys. Rev. C **62**, 045201 (2000).
27. J. P. Hilbert, N. Black, T. Barnes, E. S. Swanson, Phys. Rev. C **75**, 064907 (2007).
28. J. Haidenbauer, G. Krein, U. G. Meissner, A. Sibirtsev, Eur. Phys. J. A **33**, 107 (2007).
29. R. Röhrich *et al.*, *Technical Status Report on the Compressed Baryonic Matter Experiment*, http://www.gsi.de/documents/QCD_CBM-report-2005-001.html
30. P. González, J. Vijande, A. Valcarce, H. Garcilazo, Eur. Phys. J. A **29**, 235 (2006).
31. S. E. Koonin, D. C. Meredith, *Computational Physics*, (Addison-Wesley, New York, 1990).
32. W. -M. Yao *et al.*, J. Phys. G **33**, 1 (2006) and 2007 partial update for 2008.
33. D. Hadjimichef, J. Haidenbauer, G. Krein, Phys. Rev. C **63**, 035204 (2001); D. Hadjimichef, J. Haidenbauer, G. Krein, Phys. Rev. C **66**, 055214 (2002).
34. T. Barnes, E. S. Swanson, Phys. Rev. D **46**, 131 (1992).
35. E. S. Swanson, Ann. Phys. (NY) **220**, 73 (1992).
36. A. Valcarce, H. Garcilazo, F. Fernández, P. González, Rep. Prog. Phys. **68**, 965 (2005).
37. J. M. Cornwall, Phys. Rev. D **26**, 1453 (1982).
38. K. D. Born, E. Laermann, N. Pirch, T. F. Walsh, P. M. Zerwas, Phys. Rev. D **40**, 1653 (1989).
39. G. S. Bali *et al.*, Phys. Rev. D **62**, 054503 (2000); B. Bolder *et al.*, Phys. Rev. D **63**, 074504 (2001); P. Pennanen, C. Michael, hep-lat/0001015; C. W. Bernard *et al.*, Phys. Rev. D **64**, 074509 (2001).
40. F. Karsch, M. -T. Mehr, H. Satz, Z. Phys. C **37**, 617 (1998).